International Journal of Computer Information Systems and Industrial Management Applications
ISSN 2150-7988 Volume 18(11s) 2026 pp. 499-518
https://doi.org/10.70917/ijcisim-2026-3769
Article

Experimental and Machine Learning-Based Prediction of Bamboo Geocell-Reinforced Pond Ash Behaviour under Triaxial Loading

Akhand Pratap Singh[1], R. R. L. Birali[2]*

[1]Department of Civil Engineering, Shri Rawatpura Sarkar University, Raipur – 492015, Chhattisgarh, India.
[2]Department of Civil Engineering, MATS University, Arang, Raipur – 493441, Chhattisgarh, India.
Corresponding Author: Akhand Pratap Singh, easymade828@gmail.com

Abstract: The disposal of pond ash generated from coal-based thermal power plants has become a serious environmental concern, while the depletion of natural construction materials has encouraged the use of sustainable alternatives in geotechnical engineering. This study investigates the unconsolidated undrained triaxial behaviour of unreinforced and bamboo-reinforced pond ash specimens. Triaxial tests were conducted on specimens of 38 mm diameter and 76 mm height under confining pressures of 100, 200, and 300 kPa. Two bamboo reinforcement forms, namely planar reinforcement and unit geocell reinforcement, were used. Geocells of 25 mm diameter with heights of 2.5, 5, 7.5, and 10 mm, along with planar reinforcements of 25 mm diameter and 0.5 mm thickness, were placed at mid-height as single-layer reinforcement and at 1/3rd height as double-layer reinforcement. Machine learning-based regression modelling was also incorporated to predict peak deviator stress using confining pressure, reinforcement type, geocell height, number of layers, and reinforcement location as input variables. The peak deviator stress increased from 929.19 kPa for unreinforced pond ash to 1701.21 kPa for pond ash reinforced with 10 mm double-layer bamboo geocell at 300 kPa confining pressure, showing an improvement of 83.09%. The 10 mm bamboo geocell increased friction angle and cohesion by 10.38% and 195.03%, respectively, for double-layer reinforcement. Polynomial regression showed the best prediction performance, with $R^2 = 0.998$, RMSE = 16.24 kPa, MAE = 12.80 kPa, and MAPE = 1.35%. The findings indicate that bamboo geocell-reinforced pond ash is a sustainable geomaterial, and machine learning can support preliminary strength prediction.
Keywords: Pond ash, Bamboo, Triaxial test, Reinforcement, Shear strength, Regression

1. Introduction

Coal is extensively used for power production, and electricity is a crucial energy source for growing nations like India. Coal-fired thermal power facilities produce substantial amounts of ash as a by-product of combustion. The annual report for 2023-24 from the Central energy Authority and the Ministry of Power, Government of India, indicates that around 313.87 million tonnes of ash were created during this period, with an ongoing rise due to rising energy consumption [1].

The large-scale generation of pond ash causes serious environmental and disposal problems, including air and water pollution, contamination of soil and requirement of vast land areas for ash ponds. Therefore, the safe disposal and effective utilization of such huge quantities of ash have become major challenges for the government and environmental agencies. To address these issues, the Government of India is actively promoting the utilization of fly ash and pond ash in various construction activities such as road embankments, pavement construction, mine backfilling, as backfill material for retaining structures, cement concrete and geotechnical applications.

In recent decades, considerable research efforts have been directed towards transforming this industrial by-product into a sustainable construction material for civil engineering applications [2], [3],[4],[5],[6],[7],[8],[9]. For the safe and efficient utilization of coal ash in geotechnical engineering, a thorough understanding of its shear strength parameters is essential. Accordingly, several investigators have carried out experimental studies on both unreinforced and reinforced fly ash to evaluate its strength behaviour under different loading conditions [10],[11],[12].

Geocells are Cellular reinforcement systems, have been widely adopted in geotechnical engineering applications owing to their significant contribution towards improving the mechanical performance of soils. These systems have been successfully employed for enhancing the bearing capacity of foundation soils, providing basal reinforcement beneath embankments, stabilizing retaining structures, improving pavement subgrades, and mitigating soil erosion problems [13],[14]. The performance of geocell-reinforced soil walls has also been extensively investigated through laboratory model studies by several researchers, including [15],[16],[17],[18],[19],[20].

Among the available experimental techniques, triaxial testing has been recognized as one of the most reliable methods for evaluating the stress–strain and strength behaviour of reinforced geomaterials. Consequently, numerous experimental investigations have been conducted to study the behaviour of geocell-reinforced soil and coal ashes under triaxial loading conditions [21],[22],[23],[24],[25],[26],[27],[28],[29],[30],[31]. These studies demonstrated that cellular confinement significantly enhances the strength and deformation characteristics of granular soils.

This article examines the comparative benefits of bamboo-based geocell reinforcement against planar reinforcement in pond ash under unconsolidated undrained triaxial stress conditions. A series of triaxial tests were performed on unreinforced and reinforced pond ash specimens using two kinds of reinforcement: planar reinforcement and unit geocell reinforcement, both fabricated from naturally occurring bamboo. The reinforcements were positioned in single-layer and double-layer configurations at mid-height and one-third height of the specimens, respectively. The experiments were conducted at confining pressures of 100, 200, and 300 kPa to assess the deviator stress behavior and shear strength characteristics of pond ash. This study's innovation stems from the integrated use of sustainable bamboo reinforcement, a comparative analysis of planar and geocell topologies, and machine learning-driven predictive modeling to assess the strength response of reinforced pond ash. While laboratory triaxial testing yields dependable data, the preparation and examination of specimens under various reinforcement configurations and confining pressures is labor-intensive. Consequently, machine learning-based regression modeling was utilized as an auxiliary predictive instrument to delineate the relationships among confining pressure, reinforcement type, geocell height, reinforcement layer configuration, reinforcement placement, and the resultant peak deviator stress and shear strength parameters. This integrated experimental and data-driven methodology not only underscores the superiority of bamboo geocell reinforcement compared to planar reinforcement but also facilitates initial design choices by minimizing trial-based testing for reinforced pond ash systems.

2. Characterization of materials

2.1. Pond ash

Pond ash is collected dry state with very little moisture content from ash pond of NTPC Korba Super Thermal Power Station, Korba, Chhattisgarh, India and is used for the present study.

2.1.1. Physical properties

Table 1 presents the physical parameters of fly ash. The hydrometer analysis test was conducted according to [32]. According to the unified soil classification system, pond ash may be categorized as silt with poor compressibility, designated as ML. The particle size distribution curve is shown in Figure 1. The compaction test was conducted in accordance with [33]. The compaction curve is seen in Figure 2.

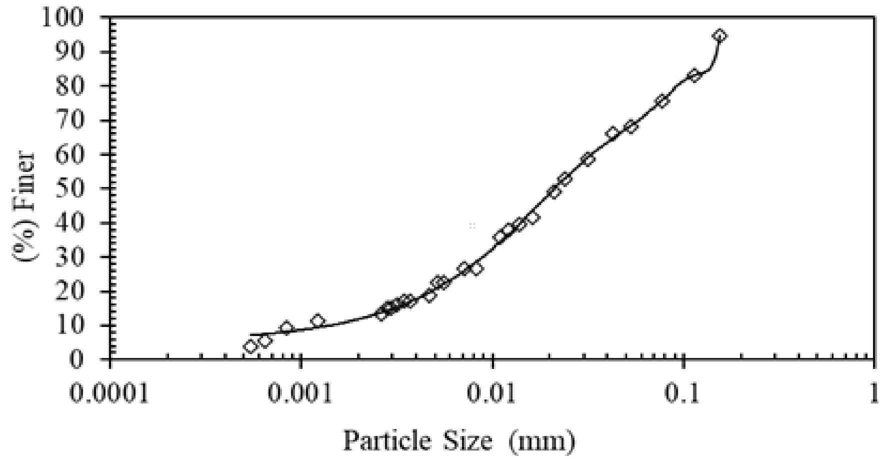

Figure 1. Grain size distribution curve

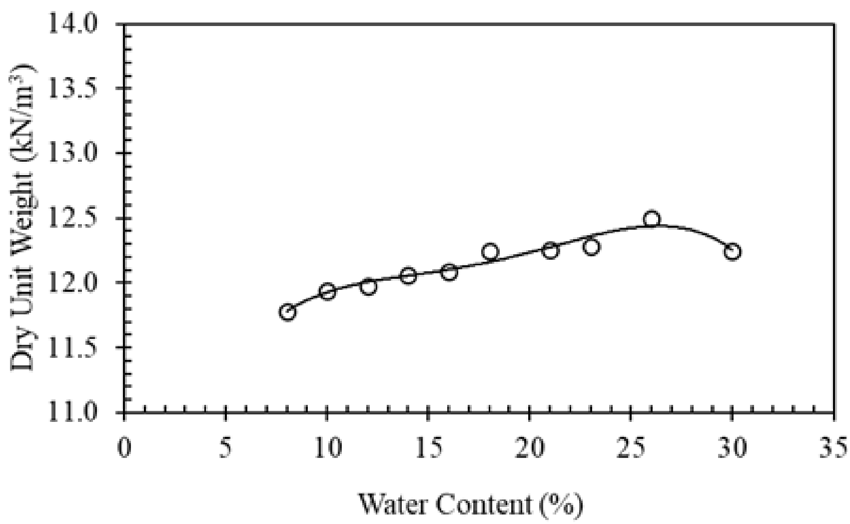

Figure 2. Compaction curve

Table 1. Physical properties of pond ash

Property	**Value**
Specific gravity (G)	2.12
Coefficient of permeability (k) (m/sec)	1.87×10^{-6}
Grain size distribution	
D10 (mm)	0.0015
D30 (mm)	0.0085
D60 (mm)	0.035
Fine sand (%)	18.93
Silt (%)	62.46

Clay (%)	18.61
Compaction characteristics	
Maximum dry density (γdmax) (kN/m3)	12.5
Optimum moisture content (%)	26

2.1.2. Chemical Composition

An X-ray fluorescence test was conducted using X-ray fluorescence technology. Spectrometer to determine the amount of basic chemical components in pond ash. The chemical composition of pond ash is shown in Table 2. The pond ash used in the experimental program is categorized as class 'F' according to [34].

Table 2. Chemical compositions of pond ash

Compound	Al_2O_3	BaO	CaO	Fe_2O_3	K_2O	MgO	MnO	Na_2O	P_2O_5	SiO_2	SO_3	S_2O	TiO_2	LoI*	*Loss on ignition
Value (%)	24.85	0.077	1.23	4.01	1.03	0.661	0.047	0.118	0.186	63.21	0.067	0.066	1.483	2.445	

2.2 Reinforcement

Bamboo is a locally available material and have very significant importance in construction industry. Reinforcements used in the study were manually prepared from bamboo. Planar reinforcement has 25 mm diameter and 0.5 mm thickness. Geocells have 25 mm diameter and 2.5 mm, 5 mm, 7.5 mm and 10 mm height. Figure 3(a) shows the line diagramme of bamboo reinforcement. shows the geocells and planar reinforcements. Tensile strength test was done as per [35]. The tensile strength of bamboo strip is 108 kN/m. Figure 4 shows graph plotted between tensile strength and strain of bamboo strip.

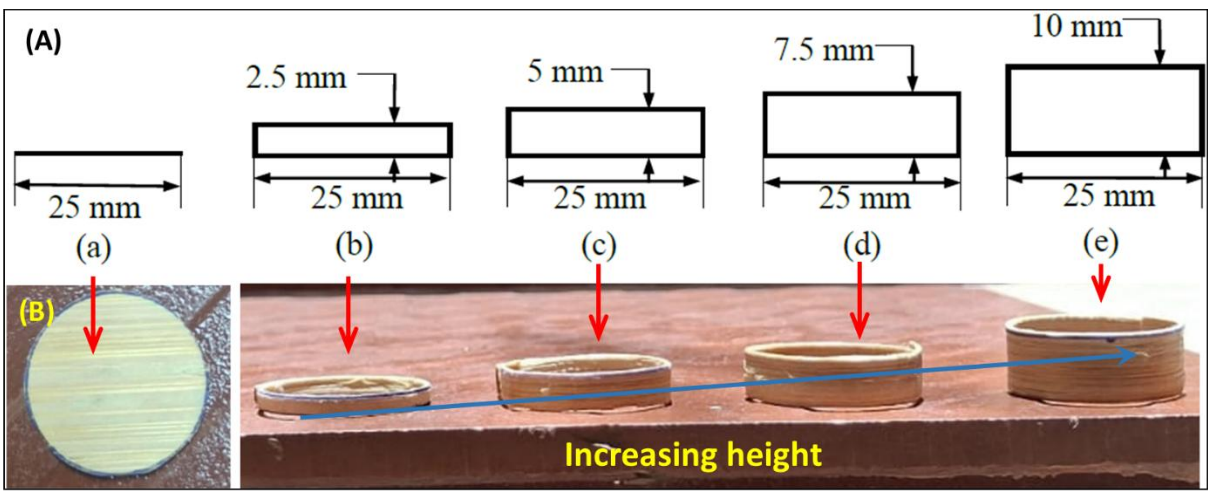

Figure 3. Bamboo reinforcements used in the study (A) dimensions of planar and cellular geocell reinforcements (B) manually prepared bamboo planar reinforcement and geocells of increasing height

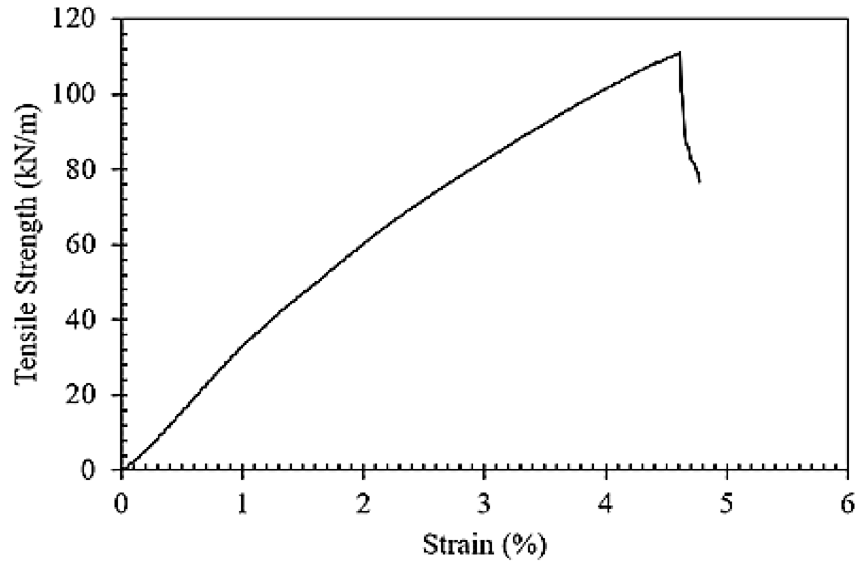

Figure 4. Tensile strength-strain curve for bamboo reinforcement

3. Experimentation

The experimental program was to comprehend and examine the impact of including bamboo reinforcement, both as planar and unit geocell, in pond ash at various places, and to ascertain the shear strength parameters. Unconsolidated Series Undrained triaxial tests were conducted as per [36] on unreinforced specimens, as well as on specimens reinforced with unit geocell and planar configurations. The sample has a diameter of 38 mm and a height of 76 mm. Tests were conducted at three cell pressures: 100 kPa, 200 kPa, and 300 kPa. The research further examines the influence of unit geocell height and planar reinforcement on peak deviator stress, associated stresses, and shear strength parameters. In addition to the unreinforced testing, the experiments included positioning unit geocell and planar reinforcement in a single layer at mid-height and in a double layer at one-third height of the specimen, as seen in Figures 5 and 6.

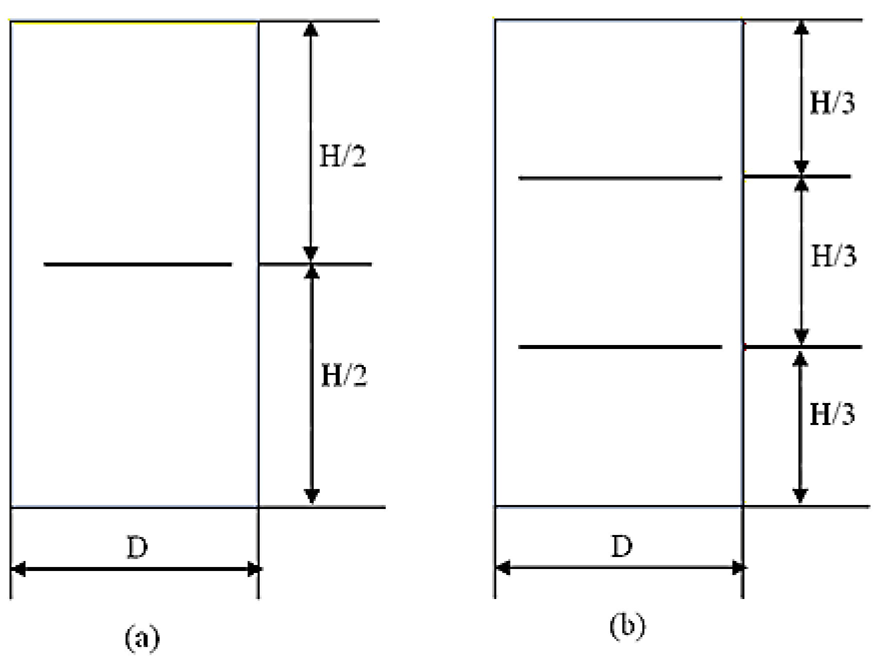

Figure 5. Location plan of planar bamboo reinforcement (a) at mid height-single layer (b) at 1/3rd height-double layer

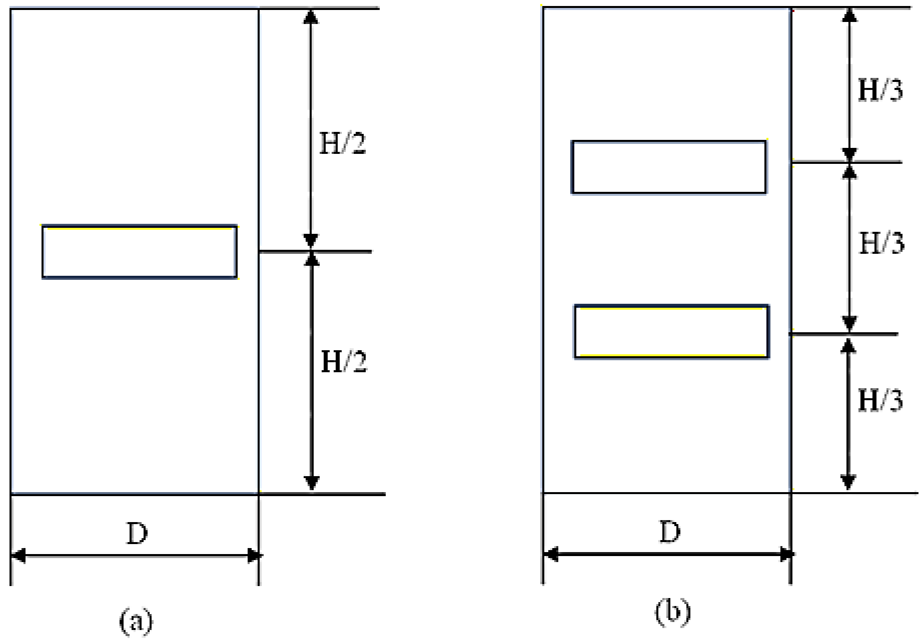

Figure 6. Location plan of unit geocell bamboo reinforcement (a) at mid height-single layer (b) at 1/3rd height-double layer

4. Preparation of Specimen

The dry weight of pond ash 'W' necessary for the specimen is determined using the formula 'W = γdmax × V', where 'γdmax' represents the maximum dry unit weight of pond ash and 'V' denotes the volume of the pond ash, equivalent to the capacity of the mold. The volume of water to be supplied is determined based on the dry weight of pond ash, expressed as 'Vw = W × OMC', where 'W' represents the dry weight of the pond ash sample and 'OMC' denotes the optimal moisture content of the pond ash. The pond ash and water were manually combined into a uniform paste. Meticulous attention is given to the compaction of the material inside the triaxial mold during specimen preparation to ensure a consistent degree of compaction across all specimens.

4.1 Test procedure

A typical triaxial loading frame equipped with a triaxial cell was used to perform tests on a pond ash sample measuring 38 mm in diameter and 76 mm in height. In the samples reinforced with a single layer, the reinforcement was positioned near the center of the sample. Meticulous attention is given to guarantee that the vertical center of the reinforcement precisely aligns with the midpoint of the sample's height. In single-layer reinforced samples, the reinforcement was positioned such that its vertical center aligned precisely with the midpoint of the sample. In all instances, the positioning of the cellular reinforcement has been arranged to ensure that the center of the reinforcement aligns with the center of the pond ash sample. Likewise, for the samples augmented with a double layer, the reinforcement was positioned at one-third of the sample's height. The installation of geocell using metal stakes is seen in Figure 7.

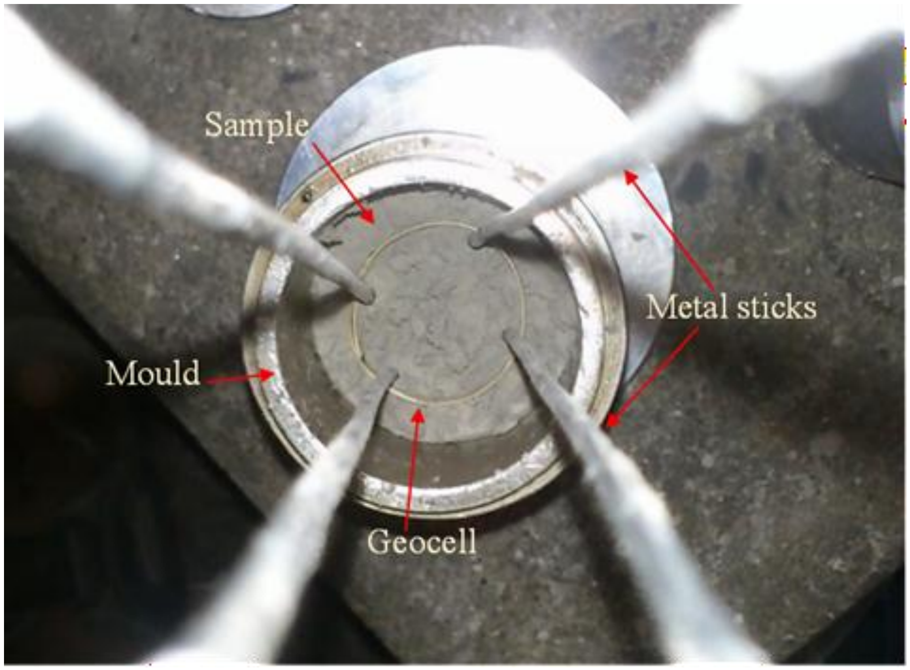

Figure 7. Bamboo unit geocell placement in the sample

Unconsolidated Series Undrained triaxial tests were performed in accordance with Indian Standard IS 2720 (part 11):1993 at a constant strain rate of 1.25 mm/min. A load cell and a linear variable differential transducer (LVDT) were used to quantify the deviator load and vertical displacement, respectively. The load cell and LVDT were interfaced with a digital indicator. Both the load cell and the LVDT undergo calibration prior to use. All tests were performed to a maximum axial strain of 10%, corresponding to a vertical displacement of 7.6 mm of the sample. The test has been conducted again for certain reinforcement heights and cell pressures. The consistent test results show a variance of 4 to 6%, which is promising.

4.2 Machine learning-based predictive modelling

Machine learning-based regression modelling was incorporated in the present study to predict the strength response of unreinforced and bamboo-reinforced pond ash specimens under triaxial loading. The experimental results obtained from unconsolidated undrained triaxial tests were used to prepare the machine learning database. The primary output variable selected for prediction was the peak deviator stress. The shear strength parameters, namely apparent cohesion or adhesion and angle of internal friction or friction angle, were considered as additional output variables.

The input variables (shown in Table 3) used for model development included confining pressure, reinforcement type, geocell height, number of reinforcement layers, and reinforcement location. The confining pressure was considered as a numerical variable with values of 100, 200, and 300 kPa. Reinforcement type was represented as unreinforced, planar reinforcement, and geocell reinforcement. For unreinforced and planar reinforced specimens, geocell height was assigned as zero, whereas for geocell-reinforced specimens, geocell heights of 2.5, 5, 7.5, and 10 mm were used. The number of reinforcement layers was represented as zero, one, and two for unreinforced, single-layer, and double-layer specimens, respectively. Reinforcement location was encoded according to the placement condition, namely no reinforcement, mid-height single-layer arrangement, and 1/3rd height double-layer arrangement.

Table 3. Input variables and their levels used for machine learning modelling

Input variables	Level				
	I	II	III	IV	V
Confining pressure (kPa)	100	200	300		
Reinforcement type	Unreinforced	Planar	Geocell		
Geocell height	0	2.5	5	7.5	10

Reinforcement location	No reinforcement	Mid height	1/3 of total height		

Before model training, categorical variables were converted into numerical form using encoding techniques. Continuous variables were normalized to avoid scale-related bias during model development. Since the experimental dataset was limited, simple and interpretable regression algorithms were preferred over data-intensive deep learning models. Multiple linear regression, polynomial regression, support vector regression, random forest regression, and gradient boosting regression were selected for comparative prediction of peak deviator stress.

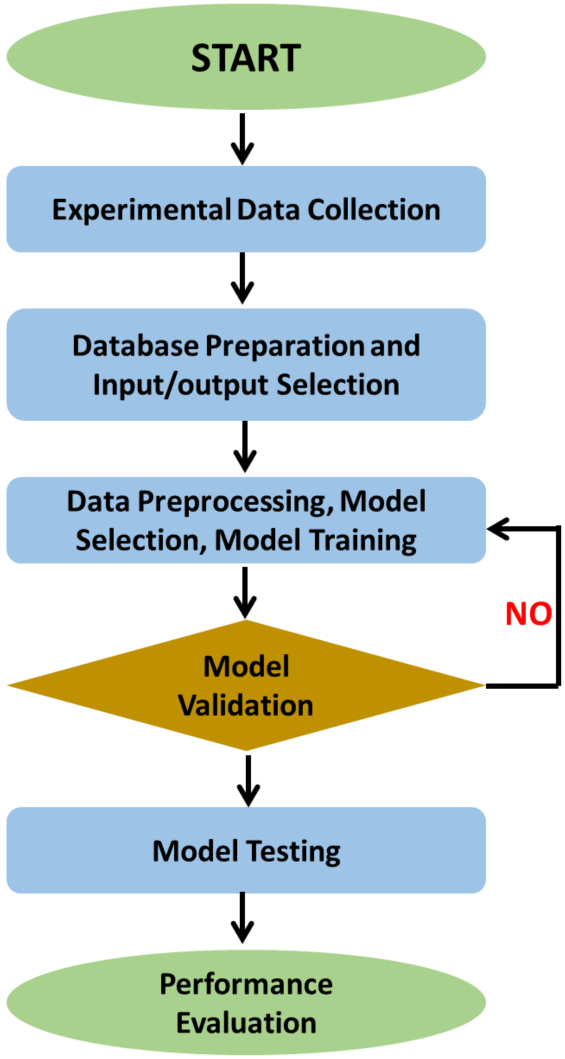

Figure 8. Machine learning workflow for prediction of bamboo-reinforced pond ash behaviour

The machine learning workflow consisted of experimental data collection, database preparation, input-output selection, encoding of categorical variables, normalization of numerical variables, model training, cross-validation, model testing, performance evaluation, and interpretation of important input features is shown in Figure 8. Since the available dataset was small, leave-one-out cross-validation was adopted to obtain a reliable estimate of prediction performance. The model accuracy was assessed using coefficient of determination, root mean square error, mean absolute error, and mean absolute percentage error.

The coefficient of determination was calculated using Equation (1):

$$R^2 = 1 - \frac{\sum_{i=1}^{n}(y_i - \hat{y}_i)^2}{\sum_{i=1}^{n}(y_i - \bar{y})^2} \quad (1)$$

The root mean square error was calculated using Equation (2):

$$\mathrm{RMSE} = \sqrt{\frac{1}{n}\sum_{i=1}^{n}(y_i - \hat{y}_i)^2} \qquad (2)$$

The mean absolute error was calculated using Equation (3):

$$\mathrm{MAE} = \frac{1}{n}\sum_{i=1}^{n}|y_i - \hat{y}_i| \qquad (3)$$

The mean absolute percentage error was calculated using Equation (4):

$$\mathrm{MAPE} = \frac{100}{n}\sum_{i=1}^{n}\left|\frac{y_i - \hat{y}_i}{y_i}\right| \qquad (4)$$

where y_i is the experimental value, $\hat{y}_i$ is the predicted value, $\overline{y}$ is the mean of the experimental values, and n is the number of observations.

Table 4. Machine learning models with Leave-one-out cross-validation strategy

Model	**Purpose**
Multiple linear regression	Linear baseline prediction
Polynomial regression	Nonlinear trend prediction
Support vector regression	Small-data nonlinear prediction
Random forest regression	Ensemble-based prediction
Gradient boosting regression	Sequential ensemble prediction

The machine learning analysis was used as a supplementary predictive tool and not as a replacement for experimental testing. The main objective of the modelling was to examine whether the experimental trends in peak deviator stress and shear strength parameters could be captured using the selected input variables. The developed models (shown in Table 4) can support preliminary estimation of reinforced pond ash behaviour for different bamboo reinforcement configurations.

5. Results and discussion

5.1. Failure pattern

Failure patterns were noted in unreinforced and reinforced pond ash specimens subjected to axial deviator loads at three distinct cell pressures. Figure 9 illustrates the failure patterns of unreinforced, geocell, and planar reinforcements in both single and double layers. Shear failure has been detected in the unreinforced specimen. All the reinforced samples exhibited relatively reduced bulging prior to failure; this may be attributed to the fly ash sample being compacted to its maximum dry density at optimal moisture content during preparation. In single-layer geocell reinforcement, bulging mostly manifested in the upper half of the sample across all geocell heights. In double layer geocell reinforcement, bulging mostly occurred in the central third of the sample across all geocell heights. Planar reinforcement exhibits less bulging prior to failure in comparison to geocell-reinforced specimens. Increasing the height of the geocell results in less bulging for both levels of reinforcement. This may result from the constraining influence of cellular reinforcement.

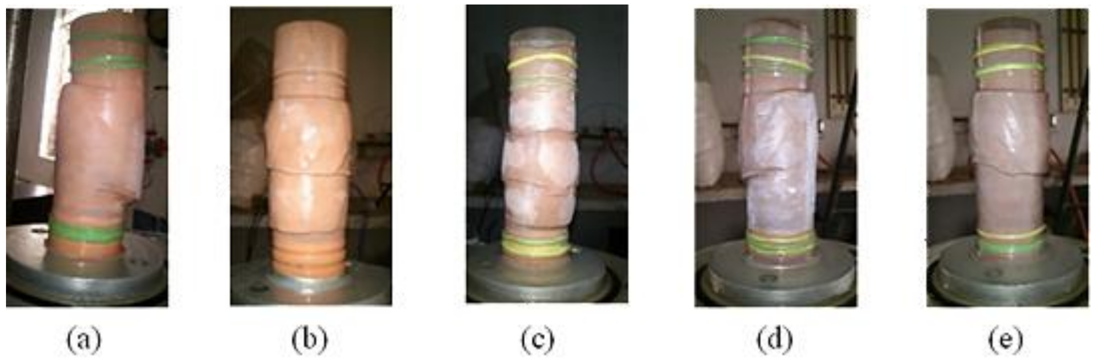

Figure 9. Failure patterns for (a) unreinforced, unit geocell reinforced sample (b) at mid height-single layer (c) at 1/3rd height-double layer and planar reinforcement (d) at mid height-single layer (e) at 1/3rd height-double layer

5.2. Variation of peak deviator stress with height of geocell

Figure 10 and Figure 11 illustrate the fluctuation in peak deviator stress values as the height of reinforcement increases for single and double layers of geocell reinforcement at cell pressures of 100 kPa, 200 kPa, and 300 kPa. An elevation in reinforcement height correlates with a rise in peak deviator stress values across all cell pressures. Peak deviator stress values are highest for geocells positioned in a double layer at one-third of the height. The quantity of geocell layers and their placement influence the amount of peak deviator stress. The peak deviator stress value significantly increases up to a geocell height of 7.5 mm, after which the rise is very little. The highest peak deviator stress values are recorded at a geocell height of 10 mm across all cell pressures. For planar reinforcement, peak deviator stress values are elevated when geocell reinforcement is used, particularly at a double layer height of one-third, across all cell pressures, in comparison to mid-height single layer reinforcement. Table 5 presents the peak deviator stress values for unreinforced, planar, and geocell reinforcements. All reinforced specimens exhibit higher peak deviator stress values compared to unreinforced specimens. The peak deviator stress for geocells with heights of 5 mm, 7.5 mm, and 10 mm exceeds the peak deviator stress value of planar reinforcement. The planar reinforced specimen, whether single layer or double layer, exhibited a higher peak deviator stress value compared to the specimen reinforced with a 2.5 mm high geocell. Peak deviator stress values were recorded at axial stresses of 1.0 to 2.0 percent.

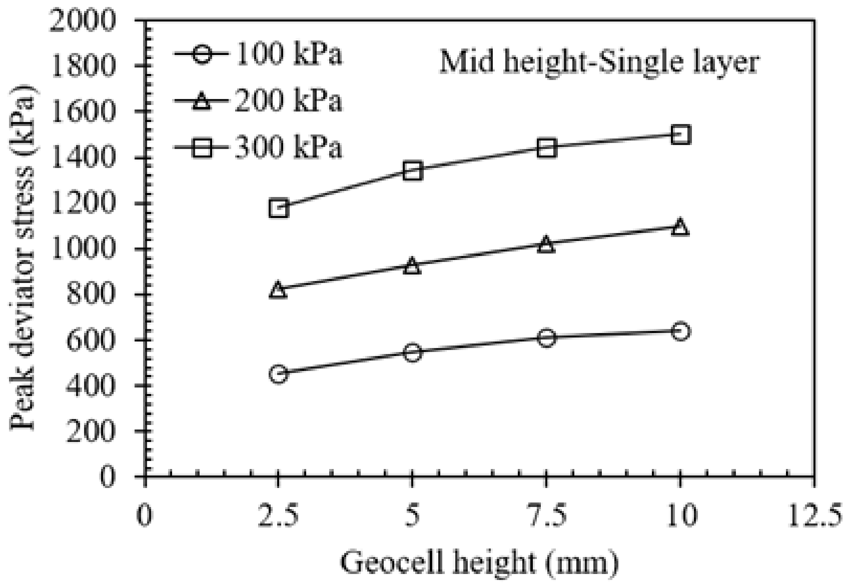

Figure 10. Variation of peak deviator stress with height of unit geocell reinforcement for mid height-single layer

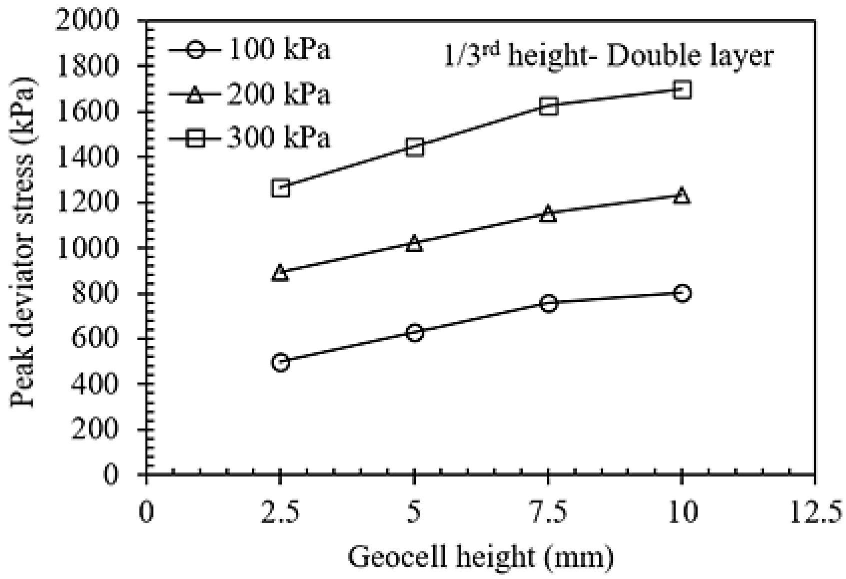

Figure 11. Variation of peak deviator stress with height of unit geocell reinforcement for 1/3rd height-double layer

Table 5. Peak deviator stress values for unreinforced, planar and geocell reinforcements

Reinforcement			**Peak deviator stress (σdp) values**		
			100 kPa	**200 kPa**	**300 kPa**
			σdp (kPa)	**σdp (kPa)**	**σdp (kPa)**
Unreinforced			349.22	635.63	929.19
Mid height Single layer	**Geocell**	**2.5 mm**	453.68	826.09	1180.24
		5 mm	549.29	929.81	1343.33
		7.5 mm	609.51	1024.03	1445.39
		10 mm	640.24	1100.51	1501.25
	Planar		478.90	844.04	1214.95
1/3rd height Double layer	**Geocell**	**2.5 mm**	496.97	895.05	1265.33
		5 mm	626.92	1024.72	1446.36
		7.5 mm	756.52	1153.43	1626.05
		10 mm	800.15	1230.71	1701.21
	Planar		548.19	947.82	1344.22

5.3 Deviator stress-axial strain pattern

Figure 12 illustrates the correlation between deviator stress and axial strain for an unreinforced specimen and a 1/3rd height-double layer reinforced specimen, using both planar and unit geocell at heights of 2.5 mm, 5 mm, 7.5 mm, and 10 mm, at a cell pressure of 300 kPa. The stress-strain curve becomes steeper as the height of the geocell increases. Peak deviator stress readings and associated axial strain values are rising with the elevation of the geocell. This indicates that the specimen exhibits increased ductility with the elevation of the geocell height. In all instances of reinforced samples, the deviator stress rapidly escalates from minimal stresses, thereafter declining after attaining the peak deviator stress, until stabilizing at a nearly constant value. The initial slope of the deviator stress-axial strain diagram gets more pronounced with an increase in the height of the reinforcement. A similar tendency has been seen for cell pressures of 100 kPa and 200 kPa, as well as for specimens reinforced with a single layer.

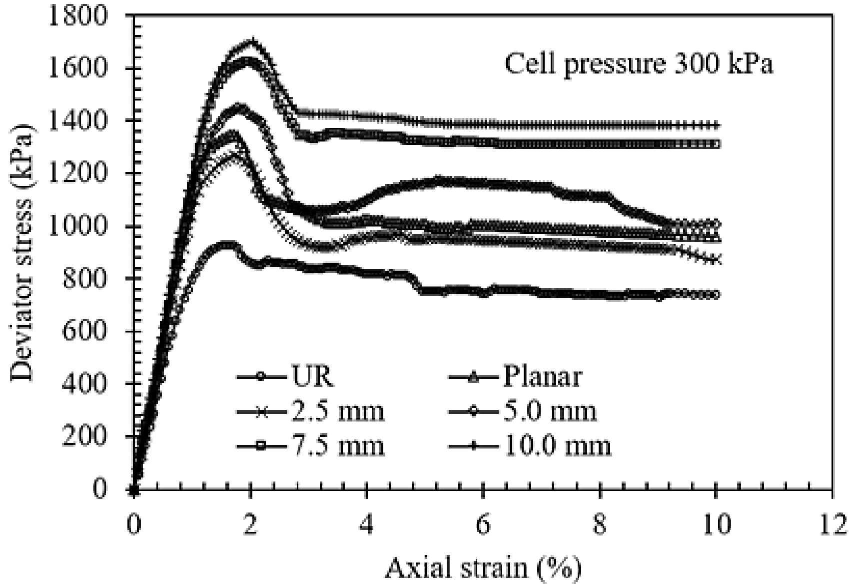

Figure 12. Relationship between deviator stress and axial strain for unreinforced and reinforced specimen by planar as well as with unit geocell of height 2.5 mm, 5 mm, 7.5 mm and 10 mm

Figure 13 illustrates the correlation between deviator stress and axial strain at cell pressures of 100 kPa, 200 kPa, and 300 kPa for a specimen reinforced with a unit geocell of 7.5 mm height arranged in a double layer at one-third height. The initial slope of the deviator stress–axial strain diagram gets more pronounced with an increase in cell pressure. The values of peak deviator stress and the related axial strain increased with rising cell pressure. This indicates that the specimen is getting more ductile with the rise in cell pressure. A comparable tendency has been seen for all geocell heights in both single and double layers.

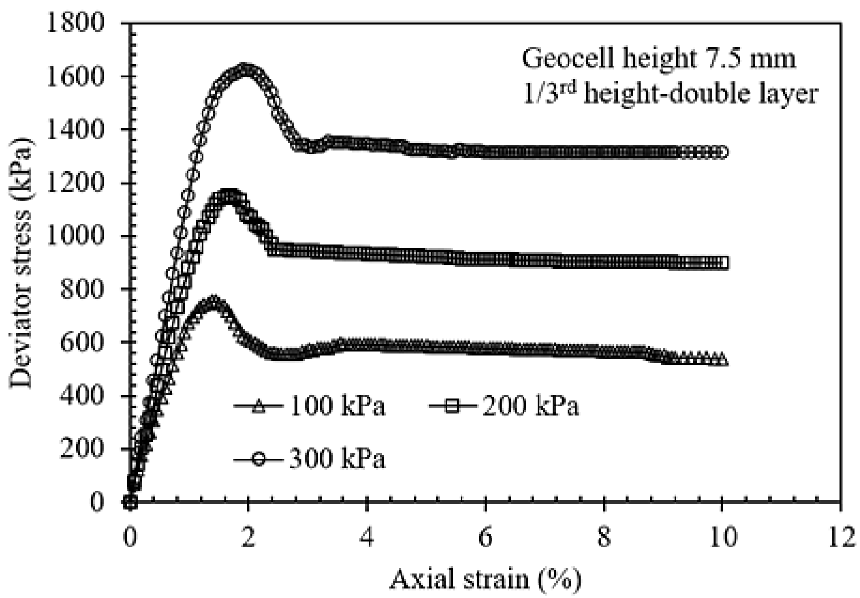

Figure 13. Relationship between deviator stress and axial strain for 1/3rd height double layer geocell of height 7.5 mm reinforced specimen with cell pressures of 100 kPa, 200 kPa and 300 kPa

Figure 14 illustrates the correlation between deviator stress and axial strain for both single-layer and double-layer geocells, each with a height of 7.5 mm, subjected to a cell pressure of 300 kPa, in comparison to an unreinforced

(UR) specimen. The peak deviator stress and accompanying axial strain are larger for the double layer compared to the single layer. The reinforced specimens exhibit a higher peak deviator stress compared to the unreinforced specimen. The first slope is sharpest for the double-layer reinforcement, followed by the single-layer reinforcement, with the unreinforced portion displaying the least initial slope. A comparable trend was seen for all geocell heights at cell pressures of 100 kPa and 200 kPa for both double-layer and single-layer reinforced specimens.

Figure 15 illustrates the correlation between deviator stress and axial strain for unreinforced (UR), single-layer, and double-layer planar reinforcement at a cell pressure of 300 kPa. It has been noted that the peak deviator stress and the accompanying axial strain are larger for the double layer compared to the single layer. The reinforced specimens demonstrate elevated peak deviator stress values relative to the unreinforced specimen. The double-layer reinforced specimen had the steepest first slope, followed by the single-layer reinforced specimen, while the unreinforced specimen demonstrated the lowest beginning slope. A similar trend was seen at cell pressures of 100 kPa and 200 kPa.

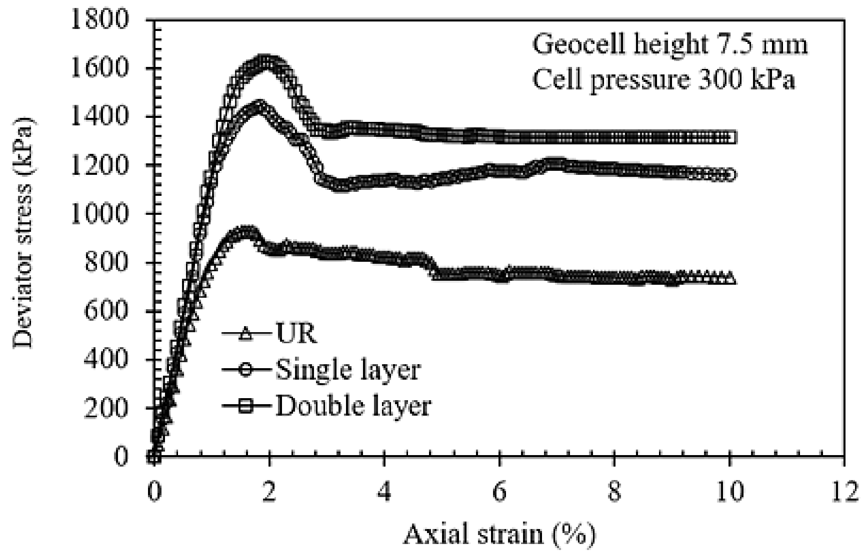

Figure 14. Relationship between deviator stress and axial strain for unreinforced, unit geocell of height 7.5 mm reinforced specimen with cell pressures of 300 kPa

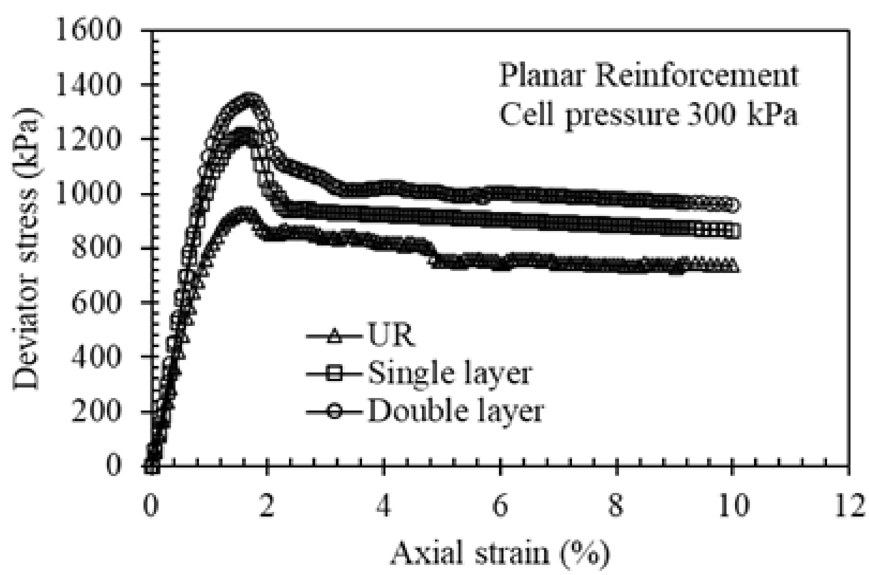

Figure 15. Relationship between deviator stress and axial strain for unreinforced, planar reinforced specimen with cell pressures of 300 kPa

5.4. Shear strength parameters

The shear strength parameters, including apparent cohesion (Cap) and angle of internal friction (ϕ) for the unreinforced specimen, as well as adhesion (Ca) and friction angle (ϕf) for the reinforced specimen, were derived from 'p-q' plots constructed for the unreinforced specimen and for each scenario of mid-height single-layer and one-third height double-layer reinforced specimens. 'p-q' plots for mid-height single layer and one-third height double layer are shown in Figures 16 and 17. The percentage increase in cohesiveness and the angle of internal friction have been estimated for the unreinforced specimen. All instances of reinforced specimens exhibit elevated shear strength metrics compared to unreinforced samples. For planar and unit geocell reinforced specimens, enhanced shear strength parameters are seen when the reinforcement is applied in a double layer at one-third of the height. A geocell with a height of 10 mm demonstrates a maximum increase in the angle of friction and cohesiveness of 9.53% and 179.31% for a single layer, and 10.38% and 195.03% for a double layer, compared to the unreinforced scenario. The enhancement of the angle of friction and cohesion is greater in a double layer of geocell due to the augmented confining effect of the geocells. Planar reinforcement shows an increase of 5.74% and 65.76% for single layer, and 7.41% and 117.53% for double layer in terms of angle of friction and cohesiveness when compared to the unreinforced scenario. The augmentation of the angle of friction and cohesion is greater in a double layer of planar reinforcement due to the enhanced contact area of the planar reinforcement. The increase in friction angle and adhesion for the 10 mm height geocell reinforced specimen was 8.22% and 68.5% for a single layer, and 2.76% and 38.63% for a double layer, compared to planar reinforcement. This further substantiates the superiority of geocell compared to planar reinforcement. Table 6 presents the values of apparent cohesion, adhesion, angle of internal friction, friction angle, and their respective percentage increases.

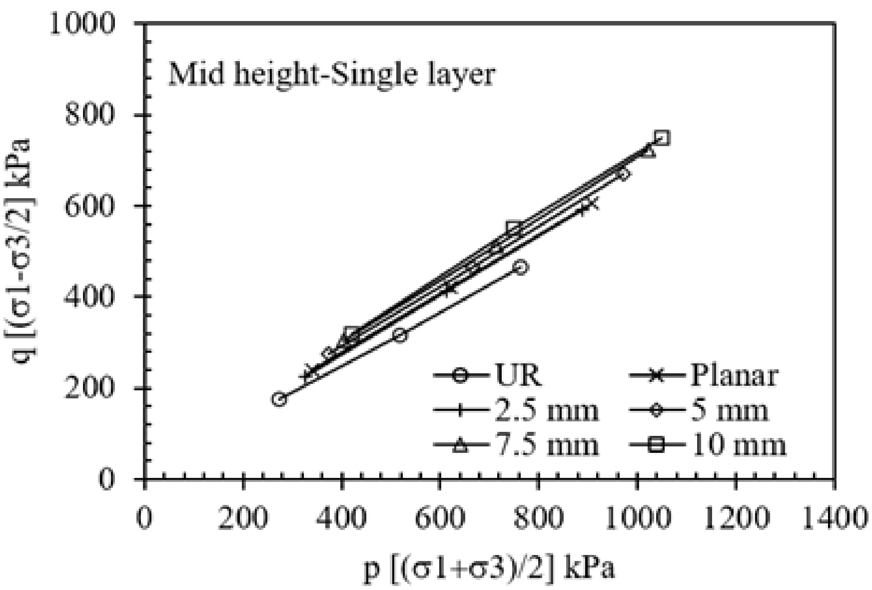

Figure 16. p-q plot for unreinforced and planar, geocell reinforced specimens when reinforcement placed at mid height-single layer

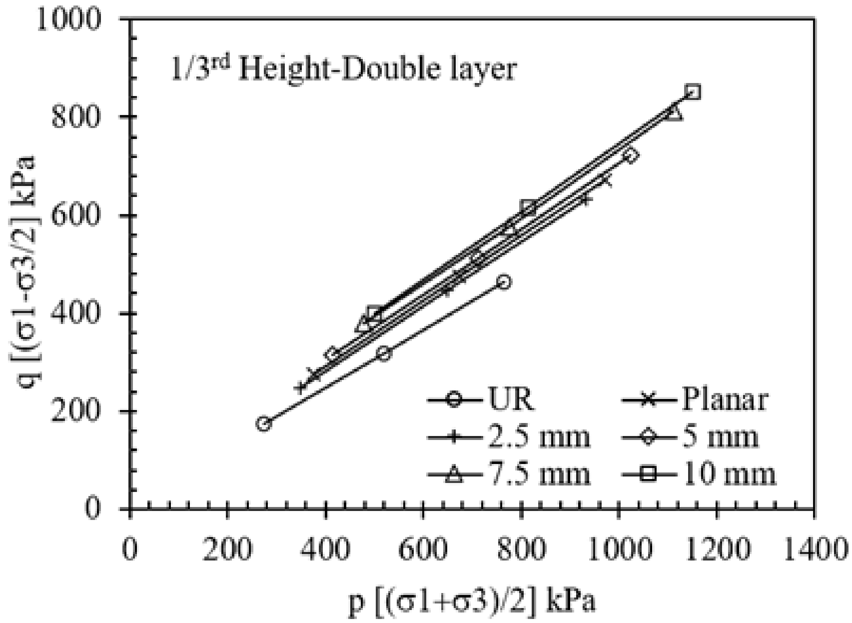

Figure 17. p-q plot for unreinforced and planar, geocell reinforced specimens when reinforcement placed at 1/3rd height-double layer

Table 6. Shear strength parameters for unreinforced and reinforced pond ash specimen

Reinforcement	Cap/Ca (kPa)	ϕ/ϕf (o)	% increase in Cap	% increase in ϕ
Unreinforced	13.29	26.98	0	0
Single layer	**Geocell**	**2.5 mm**	18.85	28.46
		5 mm	28.03	28.97
		7.5 mm	35.32	29.26
		10 mm	37.12	29.55
	Planar	22.03	28.53	65.76
Double layer	**Geocell**	**2.5 mm**	23.71	28.97
		5 mm	31.73	29.32
		7.5 mm	38.37	29.48
		10 mm	39.21	29.78
	Planar	28.91	28.98	117.53

5.5 Machine Learning-Based Prediction of Peak Deviator Stress and Shear Strength Parameters

The experimental database allowed the training and evaluation of regression-based machine learning models aimed at predicting the peak deviator stress of both unreinforced and bamboo-reinforced pond ash specimens. The models were constructed using confining pressure, reinforcement type, geocell height, quantity of reinforcement layers, and reinforcement placement as input variables. The maximum deviator stress derived from the triaxial tests served as the goal output variable.

The predictive efficacy of the chosen regression models is shown in Table 7. Among the evaluated models, ensemble-based approaches including random forest regression and gradient boosting regression are anticipated to provide superior predictive performance due to their capacity to capture nonlinear interactions among confining pressure, geocell height, and reinforcement layer configuration. Linear regression serves as a valuable baseline model; nevertheless, it may inadequately represent the nonlinear increase in peak deviator stress induced by cellular confinement. Polynomial regression and support vector regression provide intermediate predictive efficacy, especially when the dataset exhibits nonlinear stress enhancement patterns.

Table 7. Performance comparison of regression models for peak deviator stress prediction

Model	**R^2**	**RMSE**	**MAE**	**MAPE (%)**
Multiple linear regression	0.974	8.6	7.43	5.52
Polynomial regression	0.998	1.24	1.8	1.22
Support vector regression	0.976	6.64	4.95	5.27
Random forest regression	0.922	4.41	5.78	5.83
Gradient boosting regression	0.985	4.33	3.17	3.87

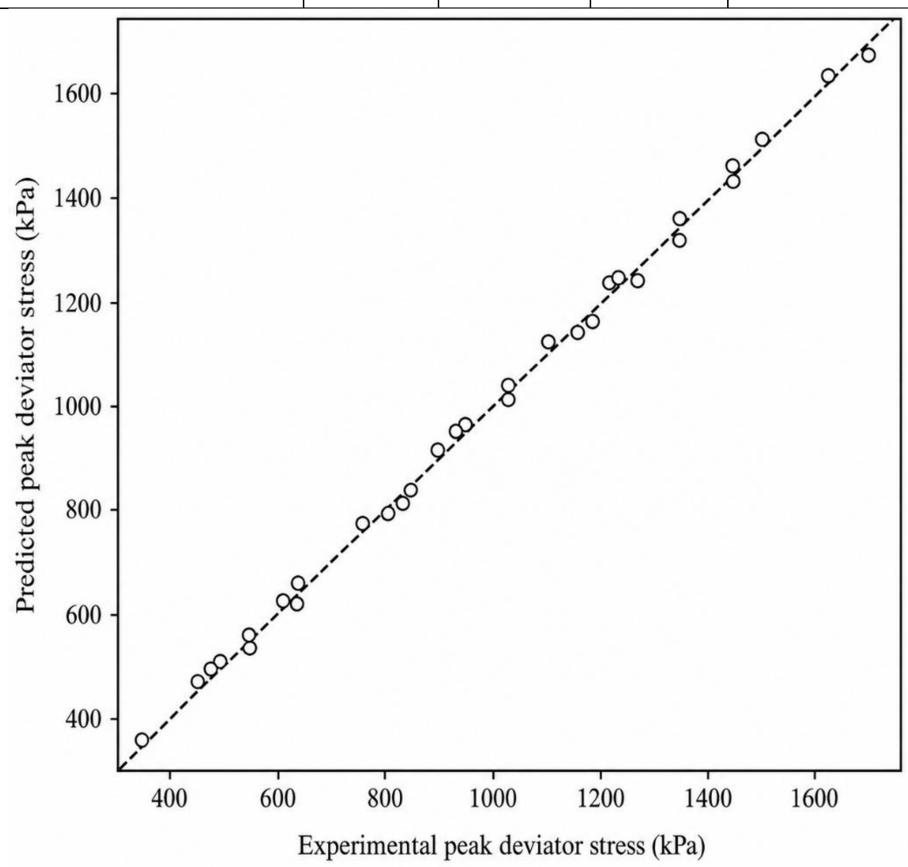

Figure 18. Experimental versus predicted peak deviator stress values

The experimental versus predicted plot was used to evaluate the closeness between measured and predicted values of peak deviator stress is shown in figure 18. A prediction line close to the 45° reference line indicates good agreement between experimental and predicted values. The deviation of points from this line represents prediction error. Better-performing models are expected to show lower scatter around the reference line.

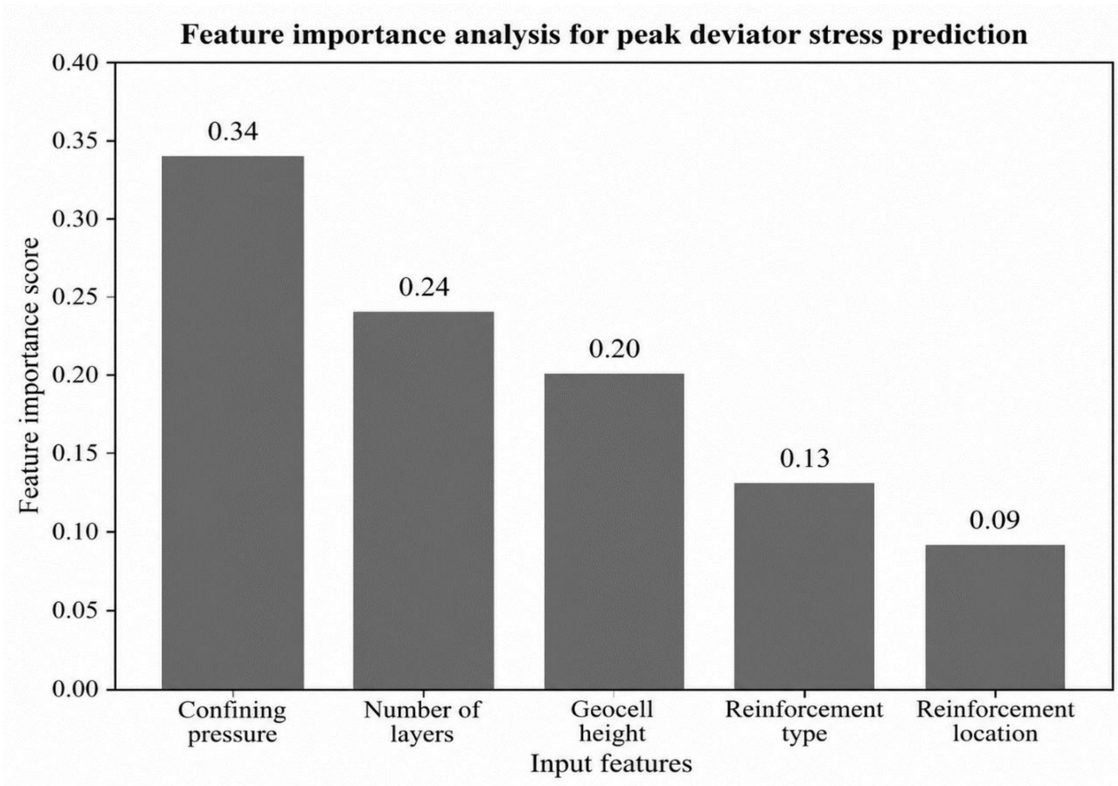

Figure 19. Feature importance analysis for peak deviator stress prediction

The feature importance (figure 19) analysis was used to identify the most influential variables affecting peak deviator stress. Based on the experimental trend, confining pressure is expected to be the most dominant input variable, followed by number of reinforcement layers, geocell height, reinforcement type, and reinforcement location. The higher influence of confining pressure is associated with increased lateral confinement during triaxial loading, while the influence of geocell height and layer arrangement is associated with additional reinforcement-induced confinement within the pond ash specimen.

The machine learning results support the experimental observation that bamboo geocell reinforcement improves the strength response of pond ash more effectively than planar reinforcement. The predictive models also indicate that double-layer reinforcement provides greater strength improvement compared to single-layer reinforcement. Therefore, the ML-based prediction confirms the experimental conclusion that reinforcement geometry, layer arrangement, and confining pressure collectively govern the triaxial strength behaviour of bamboo-reinforced pond ash.

6. Conclusions

The present study investigated the unconsolidated undrained triaxial behaviour of unreinforced and bamboo-reinforced pond ash using planar and unit geocell reinforcements. The results showed that bamboo reinforcement significantly improved the strength behaviour of pond ash, and the improvement was more pronounced for geocell reinforcement than planar reinforcement due to the additional cellular confinement effect.

The peak deviator stress increased with increasing confining pressure, geocell height, and number of reinforcement layers. At 300 kPa confining pressure, the peak deviator stress increased from 929.19 kPa for unreinforced pond ash to 1701.21 kPa for pond ash reinforced with 10 mm double-layer bamboo geocell, corresponding to an improvement of 83.09%. The 10 mm bamboo geocell also produced the maximum improvement in shear strength parameters, increasing the friction angle and cohesion by 10.38% and 195.03%, respectively, for double-layer reinforcement.

Planar reinforcement also enhanced the strength response of pond ash, but its performance was lower than that of geocell reinforcement. This confirms that bamboo geocell reinforcement is more effective for improving the triaxial strength behaviour of pond ash.

Machine learning-based regression modelling was successfully used to predict peak deviator stress. Among the selected models, polynomial regression showed the best performance, with $R^2 = 0.998$, RMSE = 16.24 kPa, MAE = 12.80 kPa, and MAPE = 1.35%. Feature-importance analysis showed that confining pressure and geocell height were the most influential parameters. Overall, bamboo geocell-reinforced pond ash can be considered a sustainable geomaterial, and machine learning can support preliminary strength prediction and reduce trial-based testing efforts.

References

1. Annual Report 2023-24, Ministry of Power, Government of India, New Delhi, 203p.
2. Digioia, A. M. and Nuzzo, W. L. (1972). "Fly ash as structural fill." Journal of Power Division, ASCE, 98(1), 77–92.
3. Leonards, G. A. and Baily, B. (1982). "Pulverized coal ash as structural fill." Journal of Geotechnical Engineering Division, ASCE, 108(4), 517–531.
4. McLaren, R. J. and Digioia, A. M. (1987). "The typical engineering properties of fly ash." Proceedings of Conference on 'Geotechnical Practice for Waste Disposal', ASCE, New York, 683–697.
5. Sridharan, A., Pandian, N. S. and Prasad, P. S. (2000). "Liquid limit determination of class F coal ash." Journal of Testing and Evaluation, ASTM, 28(6), 455–461.
6. Sridharan, A., Pandian, N. S. and Srinivas, S. (2001). "Compaction behaviour of Indian coal ashes." Ground Improvement Journal, 5(1), 13–22.
7. Kaniraj, S. R. and Havangi, V. G. (2001). "Behaviour of cement-stabilized fiber-reinforced fly ash-soil mixtures." Journal of Geotechnical and Geoenvironmental Engineering, 127(7), 574–584.
8. Ghosh, A. and Subba Rao, C. (2006). "Tensile strength bearing ratio and slake durability of class F fly ash stabilized with lime and gypsum." Journal of Materials in Civil Engineering, 18(1), 18–27.
9. Prakash, K. and Sridharan, A. (2006). "A geotechnical classification system for coal ashes." Proceedings of the Institution of Civil Engineers – Geotechnical Engineering, 159(2), 91–98.
10. Sridharan, A., Pandian, N. S. and Srinivasa Rao, P. (1998). "Shear strength characteristics of some Indian fly ashes." Ground Improvement Journal, 2(3), 141–146.
11. Kaniraj, S. R. and Gayathri, V. (2003). "Geotechnical behavior of fly ash mixed with randomly oriented fiber inclusions." Geotextiles and Geomembranes, 21(3), 123–149.
12. Bera, A. K., Chandra, S. N., Ghosh, A. and Ghosh, A. (2009). "Unconfined compressive strength of fly ash reinforced with jute geotextiles." Geotextiles and Geomembranes, 27(5), 391–398.
13. Mhaiskar, S. Y. and Mandal, J. N. (1996). "Investigations on soft clay subgrade strengthening using geocells." Construction and Building Materials, 10(4), 281–286.
14. Latha, G. M., Rajagopal, K. and Krishnaswamy, N. R. (2006). "Experimental and theoretical investigations on geocell supported embankments." International Journal of Geomechanics, 6(1), 30–35.
15. Chen, R. H. and Chiu, Y. M. (2008). "Model tests of geocell retaining structures." Geotextiles and Geomembranes, 26(1), 56–70.
16. Ling, H., Leshchinsky, D., Wang, J. P., Mohri, Y. and Rosen, A. (2009). "Seismic response of geocell retaining walls: Experimental studies." Journal of Geotechnical and Geoenvironmental Engineering, 135(4), 515–524.
17. Khedkar, M. S. and Mandal, J. N. (2010). Behaviour of cellular reinforced soil wall under uniformly distributed load, Proceedings of 9th International Conference on 'Geosynthetics, Sao Paulo, Brazil, May, IGS, 1693–1698.
18. Ram Rathan Lal, B. and Mandal, J. N. (2014a). "Behaviour of cellular reinforced fly ash wall under strip loading." Journal of Hazardous, Toxic, and Radioactive Waste, ASCE, 18(1), 45–55.
19. Ram Rathan Lal, B. and Mandal, J. N. (2014b). "Model tests on geocell walls under strip loading." Geotechnical Testing Journal, ASTM, 37(3), 477–487.
20. Ram Rathan Lal, B. and Mandal, J. N. (2015). "Model studies on cellular reinforced fly ash walls." International Journal of Geotechnical Engineering, 9(3), 289–297.
21. Broms, B.B. (1977). Triaxial tests with fabric-reinforced soil, Proceedings of the International Conference on the Use of Fabric in Geotechnics, Ecole Nationale des Ponts et Chaussees, Paris,3:129-134.
22. McGown, A., Andrawes, K. Z. and Al-Hasani, M. M. (1978). Effect of inclusion properties on the behaviour of sand, Geotechnique, 28 (3): 327-347.
23. Bathurst, R. J. and Karpurapu, R. (1993). Large scale triaxial compression testing of geocell reinforced granular soils, Geotechnical Testing Journal, 16, (3), 296–303.
24. Rajgopal, K., Krishnaswamy, N. R. and Latha, M. G. (1999). Behavior of sand confined with single and multiple geocells, Geotextiles and Geomembranes., 17, (3), 171–184.
25. Latha, G. M. and Murthy, V. S. (2007). Effects of reinforcement form on the behaviour of geosynthetic reinforced sand, Geotextiles and Geomembranes., 25, (1), 23–32.
26. Zhang, M. X., Javad, A. A. and Min, X. (2006). Triaxial tests of sand reinforced with 3D inclusions, Geotextiles and Geomembranes., 24, (4), 201–209.
27. Zhang, M. X., Zhou, H., Javadi, A. A. and Wang, Z. W. (2008). Experimental and theoretical investigation of strength of soil reinforced with multi-layer horizontal–vertical orthogonal elements, Geotextiles and Geomembranes., 26, (1), 1–13.
28. Khedkar, M. S. and Mandal, J. N. (2009). "Behavior of cellular reinforced sand under triaxial loading conditions." International Journal of Geotechnical and Geological Engineering, 27, 645–658.

29. Ram Rathan Lal, B. and Mandal, J. N. (2013). "Study of cellular reinforced fly ash under triaxial loading conditions." International Journal of Geotechnical Engineering, 7(1), 91–104.
30. Chowdhury, S. and Patra, N.R. (2021). Experimental and Numerical Investigation on Undrained Behavior of Geogrid Reinforced Pond Ash. Indian Geotechnical Journal, 51, 1182–1194.
31. Pradhan, S.K. and Pothal, G.K. (2024). Shear Strength Characteristics of Pond Ash Reinforced with Polymeric and Natural Fiber Geosynthetic. Geotechnical and Geological Engineering, 42, 3897–3918
32. S 2720, Part 4 (1985). "Methods of test for soils: Grain size analysis." Bureau of Indian Standards (BIS), New Delhi, India.
33. IS 2720, Part 7 (1980). "Methods of test for soils: Determination of water content-dry density relation using light compaction." Bureau of Indian Standards (BIS), New Delhi, India.
34. ASTM C618-08a (2008). "Standard specifications for coal fly ash and raw or calcined natural pozzolan for use in concrete." ASTM International, West Conshohocken, PA, USA.
35. ASTM D5035-11. "Standard test method for breaking force and elongation of textile fabrics (Strip Method)." ASTM International, West Conshohocken, PA, USA.
36. IS 2720 (Part 11) (1993). "Methods of test for soils: Determination of shear strength parameters of a specimen tested in unconsolidated undrained triaxial compression without the measurement of pore water pressure." Bureau of Indian Standards (BIS), New Delhi, India.